

Enhanced Survival of the LINCL Mouse Following CLN2 Gene Transfer Using the rh.10 Rhesus Macaque-derived Adeno-associated Virus Vector

Dolan Sondhi¹, Neil R Hackett^{1,2}, Daniel A Peterson³, Jamie Stratton², Michael Baad², Kelly M Travis³, James M Wilson⁴ and Ronald G Crystal^{1,2}

¹Department of Genetic Medicine, Weill Medical College of Cornell University, New York, New York, USA; ²Belfer Gene Therapy Core Facility, Weill Medical College of Cornell University, New York, New York, USA; ³Department of Neuroscience, Rosalind Franklin University of Medicine and Science, The Chicago Medical School, North Chicago, Illinois, USA; ⁴Division of Transfusion Medicine, Department of Pathology and Laboratory Medicine, University of Pennsylvania School of Medicine, Philadelphia, Pennsylvania, USA

Late infantile neuronal ceroid lipofuscinosis (LINCL) is a lysosomal storage disorder caused by mutations in the *CLN2* gene and a deficiency of tripeptidyl peptidase I (TPP-I). Prior studies with adeno-associated virus (AAV) serotype 2 or 5 mediated transfer of the *CLN2* complementary DNA to the central nervous system (CNS) of *CLN2*^{-/-} mice cleared CNS storage granules, but provided no improvement in the phenotype or survival of this model of LINCL. In this study, AAV serotypes (AAV2, AAV5, AAV8, and AAVrh.10) were compared for the delivery of the same *CLN2* expression cassette. AAVrh.10, derived from rhesus macaque, provided the highest TPP-I level and maximum spread beyond the site of injection. The AAVrh.10-based vector functioned equally well in naive rats and in rats previously immunized against human serotypes of AAV. When administered to the CNS of *CLN2*^{-/-} mice, the AAVrh.10*CLN2* vector provided widespread TPP-I activity comparable to that in the wild-type mice. Importantly, the AAVrh.10*CLN2*-treated *CLN2*^{-/-} mice had significant reduction in CNS storage granules and demonstrated improvement in gait, nest-making abilities, seizures, balance beam function, and grip strength, as well as having a survival advantage.

Received 5 July 2006; accepted 2 October 2006; published online 19 December 2006. doi:10.1038/sj.mt.6300049

INTRODUCTION

Late infantile neuronal ceroid lipofuscinosis (LINCL, a form of Batten Disease) is an autosomal recessive lysosomal storage disorder that results in progressive neurological degeneration.^{1,2} LINCL is caused by mutations in the *CLN2* gene that result in the deficiency of tripeptidyl peptidase I (TPP-I), a lysosomal enzyme that is responsible for degrading membrane proteins.^{3,4} Neurons are particularly sensitive to the lysosomal accumulation

of storage material, and individuals with LINCL have extensive, progressive neurodegeneration in all parts of the brain, resulting in a vegetative state and death by the age of 8–12 years.^{1,2}

Direct transfer of the normal *CLN2* coding sequence to the central nervous system (CNS) is one strategy for achieving sustained TPP-I expression levels in brain.^{5–7} Adeno-associated viral vectors (AAV) are ideally suited for this purpose, as they infect neurons and provide persistent expression.^{5,6,8–15} We have previously demonstrated that human-derived AAV serotypes 2 and 5 vectors encoding *CLN2* provide long-term expression of TPP-I in the CNS of *CLN2*^{-/-} mice, and reduce the numbers of lysosomal storage granules in the CNS. However, a sustained improvement in function or survival of the knockout mice was not observed suggesting that insufficient amounts of TPP-I were present.⁷

In developing a strategy to enhance the ability of AAV vectors to treat CNS-related neurodegenerative disorders, we hypothesized that maintaining the same genome but changing the capsid of the vector may provide higher expression levels and wider distribution of TPP-I in the CNS. In a comparison of 25 different AAV serotypes for levels of expression following intrapleural administration,¹⁶ we observed the highest levels of expression of a secreted marker protein with AAVrh.10, a clade E, non-human primate (rhesus macaque)-derived AAV gene transfer vector. Based on this experience, and with preliminary studies showing that AAVrh.10-mediated remarkable levels of TPP-I in the CNS of normal rats, we assessed the ability of AAVrh.10 vectors to effectively deliver the *CLN2* complementary DNA (cDNA) to the CNS of *CLN2*^{-/-} mice and to produce TPP-I in sustained levels sufficient to provide significant improvement in function and survival of this murine model of LINCL. Using the same genome with AAV2-inverted terminal repeats packaged in different AAV capsids, the data shows that, on an equal dose basis, the AAVrh.10 vector gave the highest levels of TPP-I expression and provided the best spread of TPP-I beyond the immediate administration site compared to the commonly used AAV 2, 5,

Correspondence: Ronald G Crystal, Department of Genetic Medicine, Weill Medical College of Cornell University, 515 East 71st Street, S-1000, New York, New York 10021, USA. E-mail: geneticmedicine@med.cornell.edu

and 8 capsids. As AAVrh.10 is derived from a rhesus macaque, we reasoned that it might be more applicable to use in humans owing to the absence of pre-existing anti-vector immunity. Not only was AAVrh.10 able to mediate better levels and spread of the TPP-I protein in the CNS, but it also functioned equally well in naïve animals and in animals previously immunized against the human serotypes of AAV. When the AAVrh.10 vector expressing *CLN2* was administered to the CNS of *CLN2*^{-/-} mice, the AAVrh.10CLN2-treated mice showed widespread TPP-I activity that reached the levels observed in wild-type mice. Importantly, the mice receiving the AAVrh.10 vector had improvement in gait, nest-making abilities, frequency of seizures, balance beam performance, and grip strength as well as having a survival advantage.

RESULTS

Distribution and activity of TPP-I gene product by different AAV serotypes

Rats were administered with the same dose (2.5×10^9 gc (genome copy)) of a *CLN2* expression construct packaged into the capsids of AAV2, AAV5, AAV8, or AAVrh.10. Four weeks after administration of AAV2hCLN2, TPP-I-positive staining was observed with little spread from the site of injection (Figure 1a-c). In agreement with our previous report,⁶ the morphology of TPP-I-positive cells was consistent with the transduction of neurons, whereas the white matter tracts passing through the striatum were devoid of TPP-I staining (Figure 1d). Administration of AAV5hCLN2 resulted in a much wider distribution, spreading throughout the extent of the striatum in the rostrocaudal axis, and with some spread in the mediolateral axis (Figure 1e-g). As with AAV2, cells of neuronal morphology were found to express TPP-I (Figure 1h). The distribution of TPP-I staining following delivery of AAV8hCLN2 was similar to that observed with AAV5, but the density of TPP-I-positive cells was greater (Figure 1i-l). In contrast to AAV2, 5, and 8, administration of AAVrh.10CLN2 produced a very intense signal with substantial spread that filled most of the striatum except for the white matter tracts (Figure 1m-o). TPP-I-positive cells were intensely stained in cell bodies and in their proximal processes (Figure 1p).

The morphological data was complemented by TPP-I enzymatic activity assays of brain homogenate using the same dose of the four different AAV vectors. The AAV2 vector gave peak TPP-I levels that were 1.3 ± 0.4 times the endogenous level (Figure 1q). The AAV5hCLN2 vector mediated peak TPP-I activity of 1.5 ± 0.2 times and AAV8hCLN2 produced a peak activity that was 2.4 ± 0.6 times the endogenous level. By contrast, AAVrh.10CLN2 produced an activity that was 6.4–1.6 times the endogenous level. This level was significantly higher than for the AAV2 and AAV5 vectors ($P < 0.05$), but not different from that for the AAV8 vector ($P = 0.06$). As AAVrh.10 provided both a high level and a wide distribution of TPP-I, follow-up studies were focused on AAVrh.10.

AAVrh.10 is neurotropic

As neurons are primarily at risk with LINCL, it was important to show that transduction with AAVrh.10 vectors resulted in TPP-I

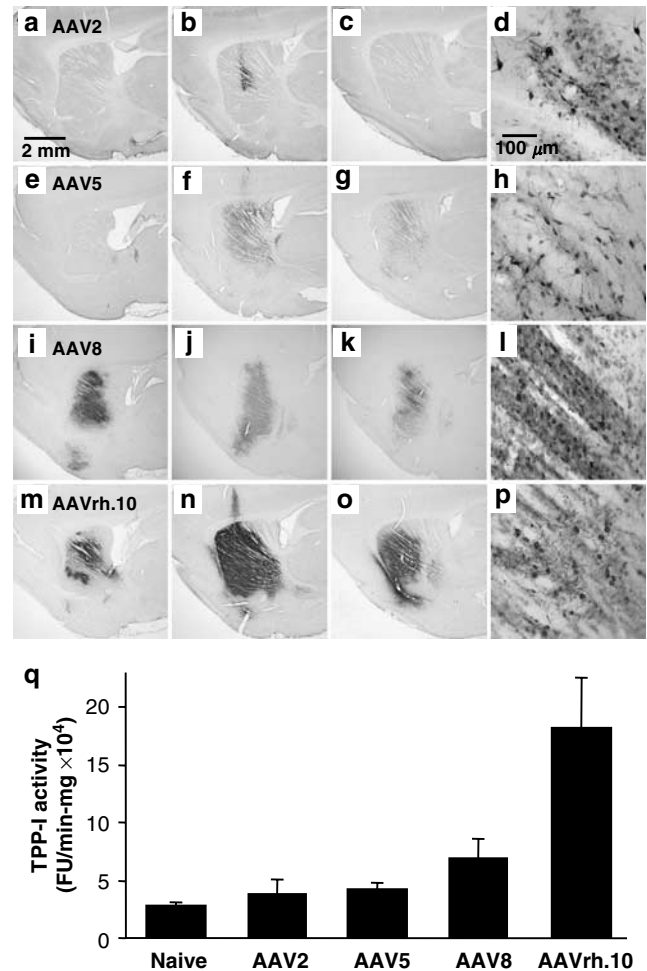


Figure 1 Comparison of TPP-I protein expression following injection of different AAV vectors expressing *CLN2* into striatum of rats. Rats ($n = 6$ /group) were injected into the striatum with 2.5×10^9 gc (in $5 \mu\text{l}$) of AAV2hCLN2, AAV5hCLN2, AAV8hCLN2, or AAVrh.10CLN2. The experiment included age-matched naïve controls ($n = 6$; not shown; all were negative). After 4 weeks, animals ($n = 3$ /group) were killed, and TPP-I distribution was assessed by immunohistochemical staining. (a-c) Series of $50 \mu\text{m}$ sagittal sections, $250 \mu\text{m}$ apart from medial to lateral, of the injected striatum for AAV2-mediated gene transfer of the *CLN2* cDNA. (d) Higher magnification showing the density of staining in the striatum resulting from gene transfer with AAV2. (e-h) AAV5, panels similar to a-d for AAV2. (i-l) AAV8. (m-p) AAVrh.10. Scale bar in a indicative of scale in a-c, e-g, i-k, m-o and scale bar in d indicative of scale in d, h, l, and p. (q) The remaining animals in each experimental group ($n = 3$ /group) were also killed at 4 weeks, the brain cut into 2 mm sagittal sections, bisected and the inner (non-cortical) material was separated and homogenized, and TPP-I activity was measured and adjusted for protein concentration. Data are mean \pm SE for the peak section corresponding to the location of vector administration.

activity in neurons. Adjacent sections were stained by multiple immunofluorescence to reveal the cell types expressing TPP-I using the mature neuronal marker, NeuN, and the astrocytic marker, glial fibrillary acidic protein (GFAP). As with the immunoperoxidase staining, TPP-I expression was observed throughout the striatum of rats except in white matter tracts (Figure 2a). Detection of coexpression by confocal microscopy revealed that TPP-I expression colocalized with neurons in the

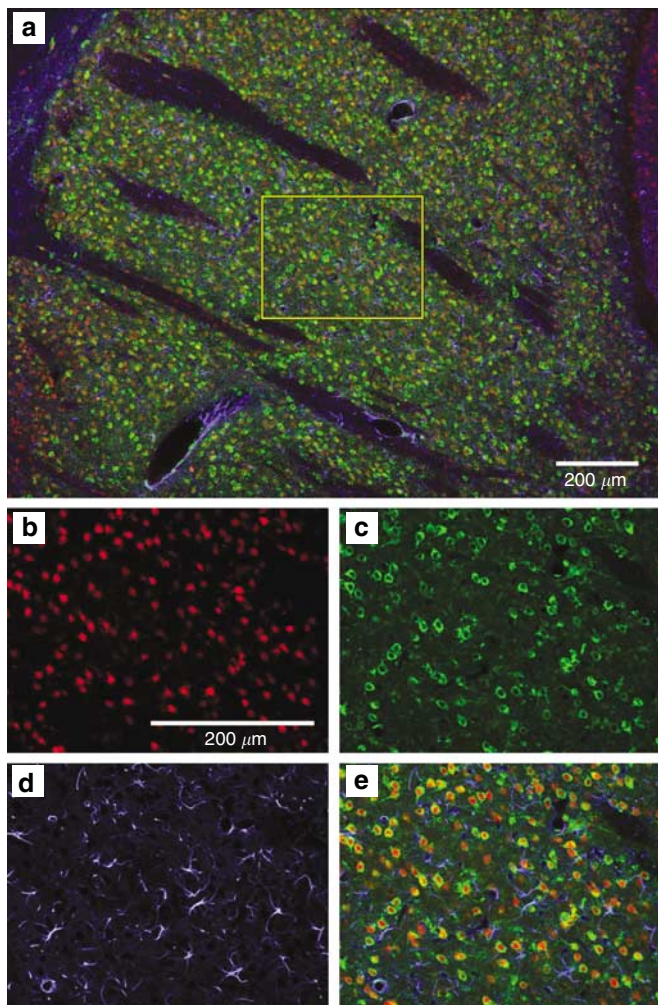


Figure 2 Preferential accumulation of TPP-I in neurons following AAVrh.10-mediated gene transfer to rat striatum. Sections of rat brain were studied by immunofluorescence 4 weeks following striatal injection of 2.5×10^9 gc of AAVrh.10CLN2. **(a)** Superimposition of the signals of TPP-I expressing cells (green) with neuron-specific staining (red, NeuN) and glial-specific staining (blue, GFAP) demonstrating neuron-specific expression mediated by the AAVrh.10 vector in the striatal region. **(b-e)** Higher power views of section outlined in **a**. **(b)** Immunofluorescent staining demonstrating neurons (red) using anti-NeuN; **(c)** immunofluorescent detection of TPP-I (green) in the same section as in **b**; **d** immunofluorescent detection of glia (blue) in the same section as in **b** using anti-GFAP antibody; and **e** superimposition of the signals of TPP-I expressing cells (green) with neuron-specific staining (red, NeuN) and glial-specific staining (blue, GFAP) demonstrating neuron-specific expression. Bar = 200 μ m (**a** and **b-e**).

parenchyma of the striatum (**Figure 2b-e**). Some expression was also noted in the endothelial cells, the choroid plexus, and the meningeal cells (not shown). Triple immunofluorescence studies using neuronal (NeuN) and glial (GFAP) markers in addition to TPP-I showed a strong colocalization of TPP-I with NeuN and no colocalization with GFAP (**Figure 2**). TPP-I cells that did not show apparent colocalization with the primarily nuclear neuronal marker, NeuN, were confirmed to be neuronal by examining adjacent focal planes. Thus, gene transfer with AAVrh.10 provides the required neuronal tropism to treat LINCL.

Projection neurons express TPP-I following striatal injection

Axonal transport may represent a powerful mechanism making use of the connections of the CNS to distribute therapeutic protein beyond the injection site. In our previous study using AAV2 vectors, retrograde transport was observed only at >2 months following gene transfer.⁶ In contrast, in serial sagittal sections examined in rats that received a single injection of AAVrh.10CLN2 into the striatum, axonal transport was readily visible at 4 weeks with strongly TPP-I-positive staining cells found in several structures with projections to the striatum including the frontal cortex, thalamus, and substantia nigra (**Figure 3a**). The intensity of TPP-I staining observed in the substantia nigra approached that seen in the injected area of the striatum. In all three of these regions, the TPP-I-positive cells were multipolar cells with the morphology of neurons (**Figure 3b-d**). To confirm the identity of these cells, adjacent sections were stained using multiple immunofluorescence. As in the striatal target region, TPP-I-positive cells in these projection regions were confirmed to be neuronal based upon their coexpression with the mature neuronal marker, NeuN, and an absence of colocalization with the astrocytic marker, GFAP (**Figure 3e-g**). This data is consistent with extensive axonal transport of vector or TPP-I protein from the site of injection.

AAVrh.10 gene delivery produces widespread expression of TPP-I

To quantitatively assess the extent of TPP-I spread following CLN2 gene transfer, volume estimates were performed comparing all serotypes of AAV (**Figure 3h**). AAV2 produced an overall TPP-I-positive tissue volume of 1.0 mm³, all of which was localized to the striatum at this vector concentration and time point. AAV5hCLN2 gene transfer produced a total TPP-I tissue volume of 10.3 mm³, of which 7.3 mm³ was within the striatum and 3 mm³ was outside. Although AAV8 staining intensity was greater than AAV5, the TPP-positive tissue volume was equivalent to AAV5. The volume of TPP-I-positive tissue for both AAV5 and AAV8 was significantly greater than for AAV2 ($P < 0.001$, both comparisons). However, AAVrh.10CLN2 gene transfer produced a total TPP-I-positive tissue volume of 19.6 mm³, of which 9 mm³ was within the striatum and 10.6 mm³ was outside. Thus, while AAV5, AAV8, and AAVrh.10 gene transfer were all able to provide TPP-I to over 75% of the rat striatum (no difference between vectors, $P > 0.05$), the AAVrh.10 vector provided a significantly larger domain of detectable TPP-I beyond the boundaries of the injected structure than either AAV5 or AAV8 ($P < 0.01$, both comparisons).

Use of non-human primate AAVrh.10 avoids problems of pre-immunity

The use of an AAV vector derived from a non-human primate may provide a therapeutic advantage by removing a barrier to gene transfer owing to pre-existing anti-vector immunity in human recipients. To assess this concept, rats were immunized against AAVrh.10 and against the three common human

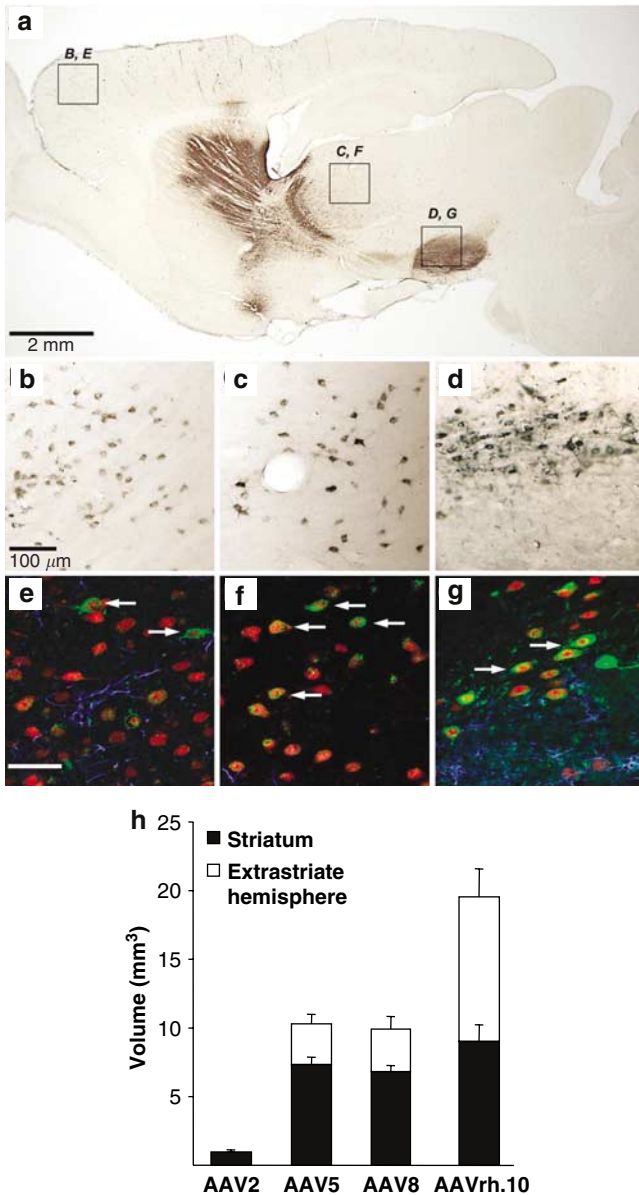


Figure 3 Distribution of TPP-I outside the striatal region of injection following AAVrh.10-mediated gene transfer to the rat CNS. Sections of rat brain were studied by immunohistochemical staining 4 weeks following striatal injection of 2.5×10^9 gc of AAVrh.10CLN2. (a) Sagittal section of the brain showing various TPP-I-positive regions outside the TPP-I-positive striatum. The TPP-I-positive regions indicated by the boxed region are magnified in the panels below; (b) frontal cortex; (c) thalamus; (d) substantia nigra. Superimposition of the signals of TPP-I expressing cells (green) with neuron-specific staining (red, NeuN) and glial-specific staining (blue, GFAP) in the (e) frontal cortex; (f) thalamus; and (g) substantia nigra. Bar = 2 mm for a, 100 μ m for b-d, and 50 μ m for e-g. (h) Volumetric analysis. Serial sections of immunohistochemically stained brains were analyzed using the Cavalieri estimator to determine the TPP-I-positive volume both within (shaded) and outside (open) the striatum. The data are the mean for $n = 3$ rats per vector.

serotypes, AAV1, 2, and 5 (Figure 4a). When the rats immunized against the human serotypes received injection of AAVrh.10 vector into the striatum, there was no difference between the vector-immunized and naïve groups ($P > 0.5$, Figure 4b). By

contrast, pre-immunization against AAVrh.10 was sufficient to reduce significantly TPP-I activity following injection of AAVrh.10 into the striatum ($P < 0.05$ compared with level in previously naïve recipients, Figure 4b).

Assessment of the impact of AAVrh.10CLN2 injection on TPP-I levels in $CLN2^{-/-}$ mice

As AAVrh.10 appeared to give better spread and higher levels of TPP-I activity after injection into the rat brain, we assessed its impact on $CLN2^{-/-}$ mice. Seven week-old mice were injected with AAVrh.10CLN2 at four locations per hemisphere. Following killing, TPP-I activity was undetected in coronal sections of the brain (Figure 5a). TPP-I activity was undetected in brain homogenates from naïve and phosphate-buffered saline (PBS)-injected $CLN2^{-/-}$ mice. Wild-type mice had a TPP-I activity of approximately 3.9×10^4 FU/min-mg, which was spatially uniform from the most rostral section to the most caudal. Injection of the $CLN2^{-/-}$ mice at four locations in each hemisphere resulted in TPP-I activities that varied from $4.7 \pm 2.2 \times 10^4$ FU/min-mg in the most rostral section to levels of $> 36 \times 10^4$ FU/min-mg in the more caudal sections. The TPP-I levels achieved in AAVrh.10CLN2-injected $CLN2^{-/-}$ mice varied from 1 to 27 times the wild-type level, depending on the location.

To further assess distribution of TPP-I activity following intracranial injection, serum and various organs of the $CLN2^{-/-}$ mice were assessed for TPP-I activity. Injection of AAVrh.10CLN2 into the brain parenchyma resulted in TPP-I activities that were greater than or equal to wild-type levels and greater than the background levels in untreated or PBS-treated $CLN2^{-/-}$ mice ($P > 0.05$, all comparisons; Figure 5b) in serum and all organs tested. The organs with the highest levels were liver > spleen > heart, kidney, lung, muscle, and serum. TaqMan realtime polymerase chain reaction established the presence of small amounts of vector in lung, spleen, and liver of some AAVrh.10CLN2-treated mice above the detection limit of < 0.05 copies/cellular genome.

Delivery of AAVrh.10hCLN2 to $CLN2^{-/-}$ mice reduces autofluorescence

To evaluate any therapeutic outcome of AAVrh.10CLN2 treatment, the extent of autofluorescence in AAVrh.10CLN2-injected and control mice was determined. Distinct cellular inclusion of lipofuscin-associated autofluorescence was observed in the striatum (Figure 6a), the thalamus (Figure 6d), and the cerebellum (Figure 6g) of $CLN2^{-/-}$ mice. In $CLN2^{-/-}$ mice receiving injections of AAVrh.10CLN2 to these regions, there was a reduction of autofluorescence in most of the field (Figure 6b, e and h, respectively). Expression of TPP-I in these regions was confirmed by immunofluorescence staining of the tissue with detection of TPP-I at a longer wavelength (not shown). Quantification of lipofuscin-associated autofluorescing particles revealed that there was a 44% reduction in the striatum (Figure 6c), 42% reduction in the thalamus (Figure 6f), and a 41% reduction in the cerebellum as a result of regional TPP-I expression (Figure 6i). These differences were significant ($P < 0.05$ compared with the untreated $CLN2^{-/-}$ mice).

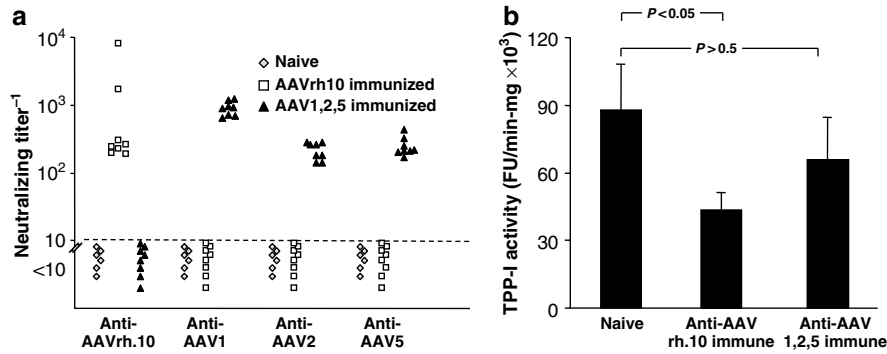


Figure 4 Impact of pre-immunization against common human AAV serotypes on gene transfer by AAVrh.10. **(a)** Neutralizing antibody titers. Six-week-old rats were injected subcutaneously at 3-week intervals with AAV1, 2, and 5, or rh.10 vectors containing irrelevant transgenes (2×10^{10} gc of AAV1lacZ, AAV2lacZ and AAV5GFP, or AAVrh.10 GFP). At 6 weeks following initial subcutaneous injection, serum anti-vector neutralizing immunity was assessed. The anti-AAV1, 2, and 5-immunized mice and the AAVrh.10 immunized mice were then administered 2.5×10^9 gc of AAVrh.10CLN2 to the CNS. **(b)** TPP-I activity. After a further 4 weeks, the brains were cut into 2 mm sagittal sections and homogenized and the TPP-I activity was determined and normalized to protein concentration. The mean and SE TPP-I activity for the peak section, at the site of injection for $n=8$ pre-immunized and $n=6$ naive rats is shown.

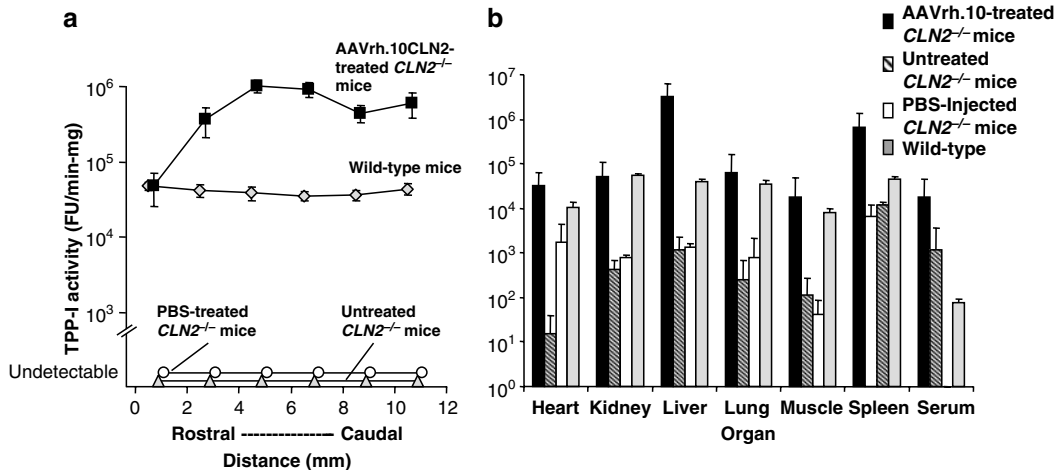


Figure 5 TPP-I activity resulting from intracranial administration of AAVrh.10CLN2 in the brain and other visceral organs of *CLN2*^{-/-} mice. Mice were injected at eight locations (bilaterally into the upper striatum, lower striatum, thalamus, and cerebellum) with either PBS or AAVrh.10CLN2 (2×10^{10} gc in 3μ l per location). When moribund, the vector- ($n=14$) or PBS-injected mice ($n=7$), the control uninjected mice (*CLN2*^{-/-}, $n=14$) and the uninjected wild-type (*CLN2*^{+/+}, $n=15$) mice were killed. **(a)** TPP-I activity in the CNS. The brain was cut into 2 mm coronal sections. Each section was homogenized, and TPP-I activity was measured and adjusted for protein concentration. **(b)** TPP-I activity in other organs. Various visceral organs were collected from the same mice, homogenized and TPP-I activity was measured and adjusted for protein concentration.

Impact of AAVrh.10CLN2 on the gait of *CLN2*^{-/-} mice

Gait analysis of mice was conducted at 18 weeks of age when the untreated *CLN2*^{-/-} mice are at their worst. In wild-type mice, the footprints for the hind paws are largely superimposed on those for the front paws and there is no dragging of the limbs (Figure 7a). In untreated *CLN2*^{-/-} mice, there was disordered gait with dragging of feet and poor coordination between the forepaw and the ipsilateral hindpaw. However, in the *CLN2*^{-/-} mice injected with AAVrh.10CLN2, there was a noticeable improvement in the coordination of the paws and reduced limb dragging.

Impact of AAVrh.10CLN2 on home cage activity of *CLN2*^{-/-} mice

In pilot experiments, the AAVrh.10CLN2-treated *CLN2*^{-/-} mice were observed to be in a better physical condition and showed

more normal activities than untreated *CLN2*^{-/-} controls which exhibited increased nest-making activity and a decrease in tremors. For nest-making activity, the wild-type mice showed consistent activity with increasing age, whereas untreated and PBS-treated *CLN2*^{-/-} mice showed decreasing activity until death (Figure 7b). AAVrh.10GFP-injected mice showed similar age-dependent reduction of nest making (not shown). By contrast, the AAVrh.10CLN2-treated mice showed a consistent pattern of nest making, with activity less than in the wild-type mice ($P<0.001$ by analysis of variance with group as factor and time as covariate), but significantly greater than in the untreated or PBS-treated *CLN2*^{-/-} mice ($P<0.001$). With regard to tremors, the wild-type mice showed no tremors at any age, whereas PBS-treated, untreated (Figure 7c) or AAVrh.10GFP-treated *CLN2*^{-/-} mice (not shown) showed more tremors with

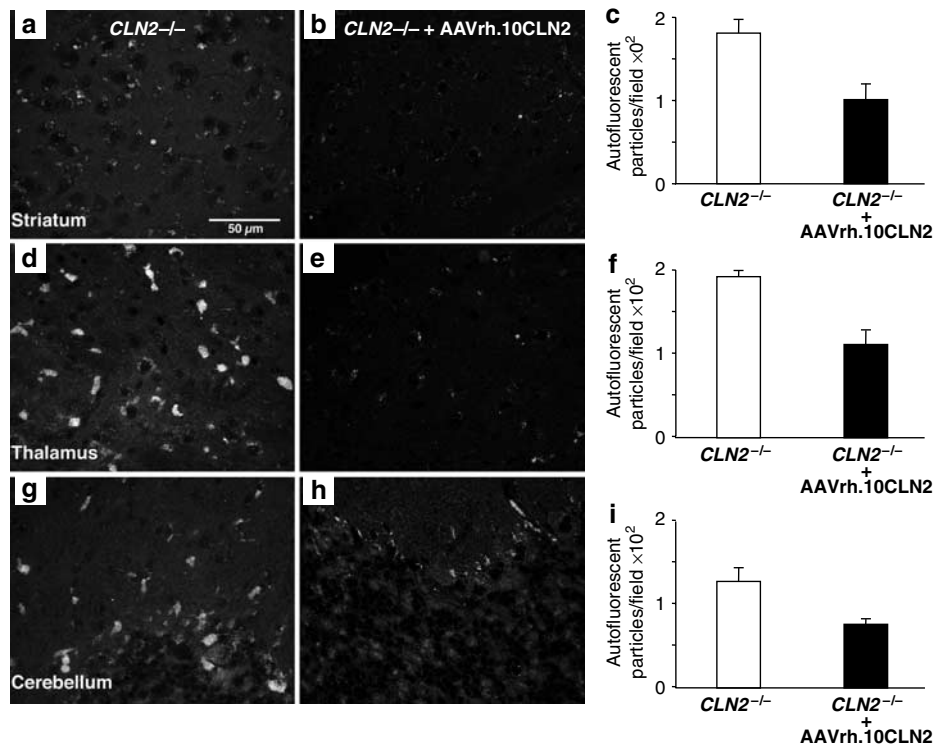


Figure 6 Lipofuscin-associated autofluorescence assessed in the CNS of $CLN2^{-/-}$ mice following CNS administration of AAVrh.10CLN2. Lipofuscin-associated autofluorescence observed in the various regions of the brain of mice that were killed owing to morbidity (~16–18 weeks for untreated $CLN2^{-/-}$ mice; 18–22 weeks for AAVrh.10CLN2-treated mice) including: (a) striatum, untreated $CLN2^{-/-}$ mice; (b) striatum, $CLN2^{-/-}$ mice treated with AAVrh.10CLN2; (c) quantitative data from striatum for naive $CLN2^{-/-}$ and AAVrh.10CLN2-treated mice; (d) thalamus, untreated $CLN2^{-/-}$ mice; (e) thalamus, $CLN2^{-/-}$ mice treated with AAVrh.10CLN2; (f) quantitative data from thalamus for naive $CLN2^{-/-}$ and AAVrh.10CLN2-treated mice; (g) cerebellum, untreated $CLN2^{-/-}$ mice; (h) cerebellum, $CLN2^{-/-}$ mice treated with AAVrh.10CLN2; and (i) quantitative data from cerebellum for naive $CLN2^{-/-}$ and AAVrh.10CLN2-treated mice. For c, f and i, quantification of lipofuscin-associated autofluorescing particles (\pm SEM) in a $1,856 \times 1,450 \mu\text{m}$ field in the various regions of the brain in the $CLN2^{-/-}$ -uninjected mice and $CLN2^{-/-}$ mice treated with AAVrh.10CLN2, and expression of TPP-1 was confirmed by immunofluorescence staining of the tissue with detection of TPP-1 at a longer wavelength (not shown).

increasing age. The AAVrh.10-treated $CLN2^{-/-}$ mice showed intermediate values with a worse tremor rating than wild-type mice ($P < 0.001$), but better tremor rating than untreated or PBS-treated $CLN2^{-/-}$ mice ($P < 0.05$).

AAVrh.10CLN2 delivery leads to improved performance in behavioral tasks

AAVrh.10CLN2-injected mice and controls were also assessed weekly for performance in tests that combine motor and sensory skills. Assessment of $CLN2^{-/-}$ mice by the balance beam test showed an age-dependent decrease in the time that the mouse could stay on the beam, from > 3 min at ages up to 12 week with a rapid decline thereafter (Figure 7d). By contrast, wild-type mice retained the ability to stay on the beam up to age > 20 week. Intracranial delivery of AAVrh.10CLN2 produced a delay in the decline of performance with age. Injection of neither PBS (Figure 7d) nor AAVrh.10GFP (not shown) impacted age-dependent deterioration. AAVrh.10CLN2-treated mice is performed better than untreated or PBS-treated $CLN2^{-/-}$ mice ($P < 0.01$, analysis of variance with age as covariate starting at week 16), although the performance of AAVrh.10CLN2-treated $CLN2^{-/-}$ mice was poorer than the performance of wild-type mice ($P < 0.01$).

Assessment of $CLN2^{-/-}$ mice by the grip strength test showed an age-dependent deterioration (Figure 7e). Wild-type mice showed strong performance on the test, which did not change with age. Injection of neither PBS nor AAVrh.10GFP (not shown) altered age-dependent deterioration. In $CLN2^{-/-}$ mice injected with AAVrh.10CLN2, there was a delay in the deterioration of performance with age ($P < 0.01$, compared to untreated or PBS-treated $CLN2^{-/-}$ mice, analysis of variance with age as covariate, commencing at week 8). The performance of AAVrh.10CLN2-treated $CLN2^{-/-}$ mice did not match that of wild-type mice ($P < 0.01$).

AAV10rh.10CLN2 delivery leads to enhanced survival in $CLN2^{-/-}$ mice

The median age of survival of the AAVrh.10CLN2-injected $CLN2^{-/-}$ mice was 162 days compared with 128 days for the uninjected $CLN2^{-/-}$ mice, 117 days for PBS-injected $CLN2^{-/-}$ mice (Figure 8), and 119 days for the AAVrh.10GFP-injected $CLN2^{-/-}$ mice (not shown). Kaplan–Meier analysis suggested that injection with PBS marginally decreased survival (the PBS-treated $CLN2^{-/-}$ mice had a significantly shorter lifespan than the untreated $CLN2^{-/-}$ mice, $P < 0.05$). In contrast, the AAVrh.10CLN2-injected $CLN2^{-/-}$ mice exhibited a significant

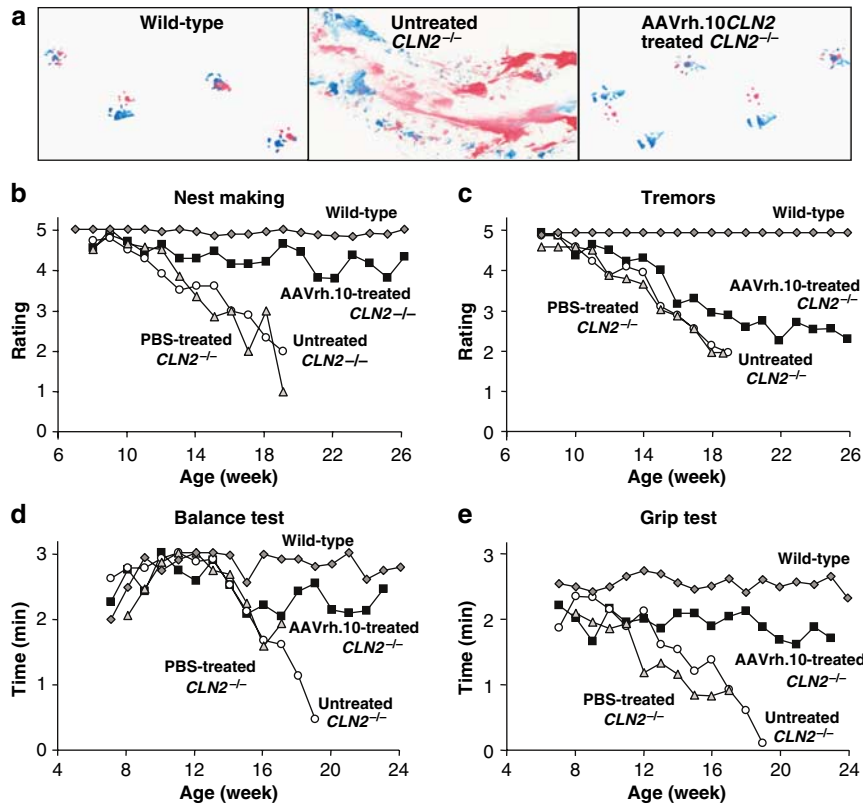


Figure 7 Impact of AAVrh.10CLN2 administration on phenotype of *CLN2*^{-/-} mice. Mice were assessed weekly after administration of vector or PBS at 7 weeks of age. **(a)** Gait analysis. The front feet of each mouse were dipped in red ink and the rear feet were dipped in blue ink. The mouse was placed at the light end of a tunnel over a sheet of white paper. As the mouse runs to the dark end of the tunnel, the footprints are recorded. Representative examples are shown for mice of 18 weeks of age. Left: wild-type *CLN2*^{+/+} mouse; middle: untreated *CLN2*^{-/-} mouse; and right: AAVrh.10CLN2 treated *CLN2*^{-/-} mouse. **(b)** Nest making. Effect of administration of AAVrh.10CLN2 on the ability of *CLN2*^{-/-} mice to create and upkeep nests (scale 0–5, see Materials and Methods). **(c)** Tremors. Effect of administration of AAVrh.10CLN2 on tremors in *CLN2*^{-/-} mice (scale 0–5, see Materials and Methods). **(d)** Balance. Effect of administration of AAVrh.10CLN2 on performance of *CLN2*^{-/-} mice on the balance beam. **(e)** Grip strength. Effect of administration of AAVrh.10CLN2 on performance of *CLN2*^{-/-} mice on grip strength. The number of mice per group for **b** and **c** included: untreated *CLN2*^{-/-}, *n* = 14; AAVrh.10CLN2-injected *CLN2*^{-/-}, *n* = 14; PBS-injected *CLN2*^{-/-}, *n* = 14; *CLN2*^{+/+}, *n* = 16. The number of mice for **d** and **e** included: untreated *CLN2*^{-/-}, *n* = 21; AAVrh.10CLN2-injected *CLN2*^{-/-}, *n* = 20; PBS-injected *CLN2*^{-/-}, *n* = 14, and *CLN2*^{+/+}, *n* = 22.

survival advantage over the untreated *CLN2*^{-/-} and PBS-treated *CLN2*^{-/-} mice (*P* < 0.001 both comparisons).

DISCUSSION

Successful gene therapy for LINCL and other lysosomal storage disorders that affect the CNS requires neurotropic gene delivery, expression of therapeutic levels of protein for a long duration with extensive spread through the brain. Previously, we have shown that an AAV2 vector containing *CLN2* can achieve locally high levels of TPP-I for at least 18 months⁶ and can clear storage granules in the CNS of *CLN2*^{-/-} mice, but with no reported improvement in performance or mortality.⁷ In this study, we compared several AAV serotypes for TPP-I expression following CNS administration. Overall, the non-human primate-derived serotype, AAVrh.10, expressing the *CLN2* cDNA produced the highest levels and broadest distribution of TPP-I expression. Immunity to human AAV serotypes did not affect *CLN2* gene transfer by AAVrh.10CLN2, an important consideration for gene delivery in human subjects who may have been exposed to AAV. CNS delivery of AAVrh.10CLN2 to *CLN2*^{-/-} mice restored

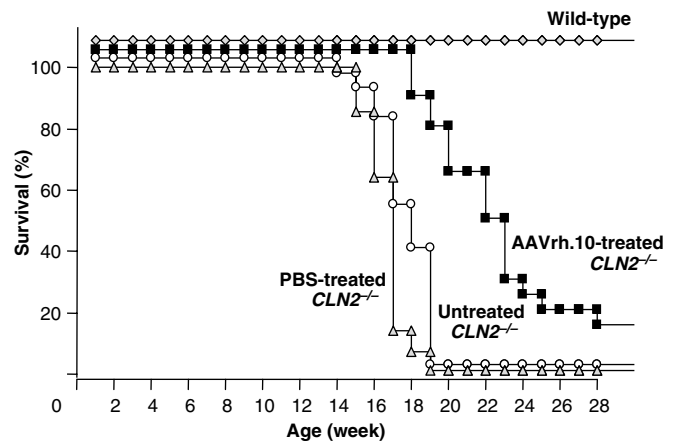


Figure 8 Impact of administration of AAVrh.10CLN2 on survival of *CLN2*^{-/-} mice. *CLN2*^{-/-} mice were administered AAVrh.10CLN2 into eight locations in the brain for a total of 1.6 × 10¹¹ gc. Survival was assessed three times per week. Any mouse that appeared moribund was killed and the age of death was recorded. The number of animals per group assessed: *CLN2*^{-/-}, *n* = 21; *CLN2*^{-/-} + AAVrh.10CLN2, *n* = 20; *CLN2*^{-/-} + PBS, *n* = 14; and *CLN2*^{+/+}, *n* = 22.

normal levels of TPP-I and reduced the accumulated autofluorescent particles in the brain. Assessment of treated *CLN2*^{-/-} mice found that delivery of AAVrh.10CLN2 significantly improved behavioral activity and performance compared to controls and, most importantly, extended survival.

Suitability of AAVrh.10 for widespread CNS delivery

Widespread expression is an important therapeutic goal for AAV-mediated gene transfer of *CLN2* cDNA. The limited extent of transduction by AAV2 vectors may result from sequestration of viral particles by adherence to their extracellular heparin-binding sites. Methods have been proposed to increase distribution by vector formulation with heparin or the simultaneous injection of mannitol to modify diffusion in the brain.¹⁷⁻¹⁹ Other serotypes of AAV offer an alternative route to wider distribution of transgene product. For example, AAV5 achieves wider distribution than does AAV2,²⁰⁻²² and improved distribution of gene transfer at the injection site has also been reported for the non-human-derived AAV serotypes AAV8,^{23,24} and recently for AAVrh.10 with a reporter gene.²⁵ The contribution of receptor binding to the enhanced distribution with the AAVrh.10 vector is unclear as the receptors are unknown.

In addition to local distribution at the delivery site, additional spread of gene product or vector by retrograde transport has been reported in the CNS following the delivery of AAV2^{6,26,27} and AAV9.²⁵ Using a single intrastriatal injection of AAV2 vector expressing *hCLN2*, we previously observed TPP-I expression in the frontal cortex 2 months post-injection, and in the thalamus and the substantia nigra, 8 months post-injection.⁶ In this study, more evidence of early retrograde transport was seen. This may reflect the overall higher expression level achieved with AAVrh.10, which is desirable provided that there is no local toxicity.

Suitability of AAVrh.10 for therapeutic use

From prior toxicology studies with an AAV2 vector and the identical expression cassette as in this study,²⁸ we know that the transgene *per se* is not toxic. One consideration for the use of AAVrh.10 vector in a clinical setting is that pre-existing antibodies to the capsid resulting from prior viral exposure could negatively impact transgene expression and/or be a risk to the patient.²⁹ The AAV2 capsid-derived peptide PADVFMVP-QYGYLTL has been identified as the dominant AAV2-induced cellular immunity-related epitope in humans who received AAV gene transfer to the hepatic artery.³⁰ This epitope is present in the capsids of multiple AAV serotypes and cellular immunity to this determinant in gene therapy subjects immune to human AAVs could theoretically result in the elimination of transduced cells. The high level of expression in AAVrh.10CLN2-treated mice previously immunized to AAV serotypes 1, 2, and 5 suggests that the cellular immunity to epitopes shared among the capsids of multiple serotypes of AAV does not lead to the elimination of transduced cells. Non-human primate-derived serotypes may be advantageous for clinical use owing to their efficiency and distribution and also by reducing the probability of attenuated gene transfer owing to pre-existing immunity. Further, considering the possibility that expression of

a therapeutic gene may not be maintained throughout the patient's lifetime, the use of non-human primate-derived AAVs may provide the option for repeat administration without immune barriers.

Intracranial delivery of AAVrh.10CLN2 to different regions of the *CLN2*^{-/-} mice resulted in elevated levels of TPP-I activity that were greater than wild-type levels, but also resulted in restoration of TPP-I levels in peripheral tissue of *CLN2*^{-/-} mice to at least the level found in wild-type mice. As the blood-brain barrier prevents TPP-I from exiting the CNS, it seems unlikely that the source of this peripheral TPP-I is from the transduced neurons. The most likely source for the peripheral TPP-I expression is the leakage of the AAVrh.10CLN2 vector into the peripheral circulation at the time of intracranial injection, and TaqMan polymerase chain reaction established the presence of small amounts of vector genome in some tissues 4 week following vector injection. This possibility is substantiated by the observation of TPP-I-positive endothelial cells, choroid plexus, and meningeal cells in brain sections. Distribution of viral particles into the vascular system could account for the detection of TPP-I activity in such diverse peripheral tissue. Theoretically, this could be an advantage, as more broad-spaced distribution of TPP-I activity is an advantage for the treatment of LINCL, which is not confined to the CNS.¹ Conversely, transvascular spread of this AAV serotype may allow some level of delivery to the brain after intravenous injection, but the doses of vector required to achieve efficiency would likely be prohibitive in regard to systemic toxicity.

The accumulation of autofluorescing particles in the perinuclear cytoplasm is an indicator of the severity of cellular toxicity in *CLN2*^{-/-} mice.^{7,31} Clearance of cellular debris is a criterion to evaluate therapeutic strategies.^{7,32} We observed a significant decline in the extent of autofluorescing particles in targeted brain regions following delivery of AAVrh.10CLN2. Whether the clearance of the storage granules represents prevention or reversal is unknown.

Effect of AAVrh.10CLN2 delivery on behavior and survival

The most important measures of therapeutic success are the improvement in overall behavioral function and survival. In our prior study, there was no improvement in performance or survival in spite of reduced cellular pathology following AAV2-mediated *CLN2* delivery to *CLN2*^{-/-} mice.⁷ Another study using AAV2-mediated delivery of the palmitoyl protein thioesterase-1 cDNA into the *CLN1*^{-/-} mice (to assess the closely related disease, infantile neuronal ceroid lipofuscinosis) found improvement in cellular pathology and a variety of activity and sensorimotor tasks, but no improvement in survival.³³ In this study, we found that delivery of the *CLN2* gene by AAVrh.10 resulted in improvements in gait, nest-building activity, tests of sensorimotor performance, and in reduced tremor compared with those of controls. The increased performance and longevity mediated by AAVrh.10 vector was afforded by treatment with AAVrh.10CLN2 at 7 weeks of age. It is possible that earlier intervention would further prevent the accumulation of pathological burden and extend performance and survival.

These results suggest that AAVrh.10 is a suitable vector for preclinical development in treatment of LINCL.

MATERIALS AND METHODS

AAV vectors. All AAV vectors contain the same expression cassette consisting of the human *CLN2* cDNA driven by a CMV/ β -actin hybrid promoter surrounded by the inverted terminal repeats of AAV2.^{6,34} 293 cells were transfected using Polyfect with the plasmid containing the AAV genome and with one or two other plasmids (see below) supplying the required adenovirus and AAV functions. After 72 h, the cells were harvested and AAV purified on iodixanol gradients, followed by heparin affinity chromatography for AAV2 or QHP ion exchange chromatography for AAV5, 8, and rh.10. Vector preparations were assessed by TaqMan real-time polymerase chain reaction to determine gc and by *in vitro* gene transfer in 293 ORF6 cells.³⁵

AAV2 vectors were produced using a helper plasmid pPAK-MA2, which contains the *rep* and *cap* genes of AAV2 and the E2, VA, and E4 helper genes of adenovirus.²⁸ AAV5 vectors were produced using a helper plasmid pDG5, which provides the adenovirus helper functions in addition to the *rep* gene of AAV2 and the *cap* gene from AAV5.³⁶ AAV8 vectors were produced by cotransfection of the vector plasmid with two helper plasmids, one (p Δ F6) with the adenovirus helper functions and the other with the AAV2 *rep* gene and the AAV8 *cap* gene.³⁷ AAVrh.10 vectors were produced by cotransfection of the vector plasmid with two helper plasmids, p Δ F6 and the other with the AAV2 *rep* gene and the AAVrh.10 *cap* gene.¹⁶

Rat experiments. For comparisons among AAV serotypes, Fischer 344 male rats (Taconic, Germantown, NY) received unilateral AAV administration into the left striatum (AP +0.60, ML +2.8, and DV -5.2). The AAV vectors (2.5×10^9 gc in PBS) were injected at a rate of 0.2 μ l/min using a microprocessor controlled infusion pump (Model 310, Stoelting, Wood Dale, IL). Rats were also used to assess AAVrh.10 *CLN2* gene transfer in the context of pre-existing immunity against human AAVs. Rats (130–150 g) were pre-immunized subcutaneously on days 0 and 21 with either AAVrh.10Luciferase (2.0×10^{10} gc), or AAV1, 2, and 5 (2.0×10^{10} gc; with nonspecific transgenes) or left as naïve controls. Forty-two days later, serum anti-AAV antibodies were determined by *in vitro* gene transfer assay.¹⁶ Rats were then injected with AAVrh.10*CLN2* (2.5×10^9 gc in 2 μ l of PBS) into the left striatum as described above.

Evaluation of TPP-I protein expression in the rat brain. TPP-I enzymatic activity was assessed in coronal sections of brain as described previously.^{6,38} Immunohistochemical detection of TPP-I distribution in brain 4 weeks after gene transfer was assessed, as described previously.^{6,38} To ensure comparability among serotypes, all sections were processed for immunohistochemistry and imaged in the identical manner. Volume was assessed by using the Cavalieri estimator.³⁹ Multiple immunofluorescence labeling was performed, as described previously^{6,38} using antibodies specific for neurons (mouse anti-NeuN, 1:2,500, Chemicon International, Temecula) or astrocytes (guinea-pig anti-GFAP, 1:500, Advanced Immunochemical, Long Beach, CA). Expression of the *CLN2* transgene product was detected using a mouse anti-human TPP-I antibody at a dilution of 1:1,000.⁴⁰

CNS administration of AAVrh.10 to *CLN2* knockout mice. Original heterozygous breeding pairs of *CLN2* knockout mice back crossed into C57Bl/6 were used to produce all of the *CLN2*^{-/-} mice used in this study.³¹ Genotypes of pups were determined by polymerase chain reaction.³¹ At 7 weeks of age, *CLN2*^{-/-} mice received administrations bilaterally in four locations per hemisphere: lower striatum (A/P +0.60 mm, M/L -1.75 mm, D/V -4.0 mm), upper striatum (A/P

+0.60 mm, M/L -1.75 mm, D/V -2.0 mm), thalamus (A/P -2.0 mm, M/L -1.0 mm, D/V -3.0 mm), and cerebellum (A/P -6.0 mm, M/L -0.5 mm, D/V -1.5 mm). *CLN2*^{-/-} mice received AAVrh.10*CLN2*, AAVrh.10 GFP (both 2×10^{10} gc), or PBS in 3 μ l volume at 0.5 μ l/min. Uninjected *CLN2*^{-/-} mice served as negative controls and *CLN2*^{+/+} served as positive controls.

Enzymatic analysis of TPP-I activity in mouse brain and organs. When mice became moribund, they were deeply anesthetized, and blood was obtained by cardiac puncture. They were transcardially perfused with PBS and the whole brain, heart, kidney, liver, lung, quadriceps, and spleen were excised. The brain was hemisected and the right hemisphere was submerged in 4% paraformaldehyde for morphological evaluation and left hemisphere was sectioned into 2 mm coronal sections and assessed for TPP-I activity, as described above for the rat brain. Each organ was also homogenized and assessed for TPP-I activity and vector DNA content by Taqman.^{6,41}

Quantification of autofluorescence in mouse brain. Image analysis was used as a measure of the abundance of autofluorescent particles in naïve and AAVrh.10-*CLN2*-injected *CLN2*^{-/-} mice. Autofluorescence was detected in sections of striatum, thalamus, and cerebellum previously stained for the presence of TPP-I by immunofluorescence. Regions containing TPP-I-Alexa488 fluorescence were imaged using UV excitation with a 460/32 emission filter to detect autofluorescence. Equivalent regions were sampled in uninjected mice. All images were collected at identical camera settings on an Optronics Magnafire-equipped Olympus BX51 using a $\times 20$ lens to sample a $1856 \times 1450 \mu$ m field of view. Image analysis was conducted by another investigator blinded to group identity with standardized settings using ImageJ (<http://rsb.info.nih.gov/ij/download.html>). The number of particles and two SDs above mean intensity was determined using a boundary area of 50–800 pixels to include lipofuscin particles within cells, but to exclude nonspecific autofluorescence.

Behavioral assessment of *CLN2* knockout mice. In three separate experimental series, cohorts of $n=7$ *CLN2*^{-/-} mice were injected, as described above, and a number of phenotypic observations were made at intervals to assess the impact of administration of AAVrh.10*CLN2* versus AAVrh.10GFP or PBS. The negative controls were untreated *CLN2*^{-/-} mice and the positive controls were wild-type mice. The assessments used and the testing intervals included (1) gait (in a subset of mice at weekly intervals), (2) nest making (weekly), (3) tremors (weekly), (4) performance of balance beam (weekly), (5) performance on grip strength test (weekly), and (6) morbidity/mortality (three times per week). All tests were performed at the same time each week and under similar conditions. Following three independent experimental series, all available datapoints were combined for statistical analysis.

Gait analysis. Gait analysis was performed with a subset of mice each week sampling all ages and all groups for comparison. A blind tunnel (100 cm long, 20 cm wide, 10 cm high) was created with a plain white paper floor. The front paws of a mouse were dipped in red paint, and back paws in blue paint (Crayola washable paints, Binney and Smith, Easton, PA). The mouse was placed in the front of the tunnel on the paper so that it could run down the tunnel to the dark end. The piece of paper with the colored paw prints was retained for qualitative analysis.

Nest making. Based on empirical observations in the first experimental series, a nest-making scale was created and applied to the second and third experimental series. Individual mice were moved to a clean cage with two cotton nestlets for weekly assessment. They were rated on a scale of 1–5 as follows: score 1, no nest was created and the nestlets remained intact; score 2, edges of the nestlets were chewed but no nest created; score 3, ~50% nestlets were chewed up but the mice were

unable to create an adequate nest; score 4, all the nestlets were chewed up but did not result in a structured nest; and score 5, the structured nest of a healthy mouse.

Tremors. Based on empirical observations in the first experimental series, a tremor scale was created and applied to the second and third experimental series. Tremors were assessed while the mouse was on the balance beam (described below) for a period of 30 s. Animals were rated on a scale of 1–5 as follows: score 1, occasional violent and severe seizures coupled with repeated tremors; score 2, tremors and shaking most of the time; score 3, tremors and shaking occasionally; score 4, a shuffling movement with splayed hind feet but no tremors or shaking; and score 5, an active and agile mouse with no visible tremors or shuffling.

Balance beam test. A horizontal polyurethane treated wooden beam 3 cm in width was affixed to a wooden stand 100 cm high, which was placed over a plastic tub filled with underpads to provide a soft landing for any mouse that fell off. The mouse was placed in the center of the wooden beam and was allowed to move along, and the time till fall was recorded. After 3 min, any mouse that had not fallen was returned to its cage, and the time was recorded as 3 min.

Grip strength. A string was stretched between two vertical wooden dowels, and a plastic tub filled with underpads was placed below. The mouse was placed in the center of the suspended string, hanging by its front paws and the time till falling was recorded. If the mouse was still hanging after 3 min, it was removed from the string and the time recorded as 3 min.

Survival. Three times per week, mice were observed and, if deemed moribund, (inactive with severe shaking and weight loss), were killed and the age of death was recorded.

Statistics. Data is presented as mean ± SE. For serotype and gene expression volume comparisons, groups were compared by analysis of variance using *post hoc* Fisher tests. For the quantification of the autofluorescent storage granules, a two-tailed Student's *t*-test was used. Behavioral assessments were performed by analysis of variance using treatment group as factor and time as covariant. Survival difference between two groups was assessed using Kaplan–Meier test.

ACKNOWLEDGMENTS

We thank P Lobel and D Sleat from University of Medicine and Dentistry of New Jersey for providing the CLN2^{+/-} breeding pairs and for valuable discussions; K Wisniewski and A Golabek from NYS Institute for Basic Research for providing the anti-hCLN2 antibody; TP O'Connor for helpful discussions; E Vassallo and C Sanders for technical assistance; and N Mohamed for help in preparing this paper. These studies were supported, in part, by U01 NS047458; Nathan's Battle Foundation, Greenwood, IN; and the Will Rogers Memorial Fund, Los Angeles, CA.

REFERENCES

- Williams, RE, Gottlob, I, Lake, BD, Goebel, HH, Winchester, BG and Wheeler, RB (1999). CLN2: Classic late infantile NCL. In: Goebel, HH (ed). *The Neuronal Ceroid Lipofuscinoses (Batten Disease)* IOS Press: Amsterdam, pp 37–53.
- Haltia, M (2003). The neuronal ceroid-lipofuscinoses. *J Neuropathol Exp Neurol* **62**: 1–13.
- Vines, DJ and Warburton, MJ (1999). Classical late infantile neuronal ceroid lipofuscinosis fibroblasts are deficient in lysosomal tripeptidyl peptidase I. *FEBS Lett* **443**: 131–135.
- Sleat, DE *et al.* (1997). Association of mutations in a lysosomal protein with classical late-infantile neuronal ceroid lipofuscinosis. *Science* **277**: 1802–1805.
- Haskell, RE, Hughes, SM, Chiorini, JA, Alisky, JM and Davidson, BL (2003). Viral-mediated delivery of the late-infantile neuronal ceroid lipofuscinosis gene, TPP-1 to the mouse central nervous system. *Gene Ther* **10**: 34–42.
- Sondhi, D *et al.* (2005). AAV2-mediated CLN2 gene transfer to rodent and non-human primate brain results in long-term TPP-1 expression compatible with therapy for LINCL. *Gene Ther* **12**: 1618–1632.
- Passini, MA *et al.* (2006). Intracranial delivery of CLN2 reduces brain pathology in a mouse model of classical late infantile neuronal ceroid lipofuscinosis. *J Neurosci* **26**: 1334–1342.
- Kaplitt, MG *et al.* (1994). Long-term gene expression and phenotypic correction using adeno-associated virus vectors in the mammalian brain. *Nat Genet* **8**: 148–154.
- McCown, TJ, Xiao, X, Li, J, Breese, GR and Samulski, RJ (1996). Differential and persistent expression patterns of CNS gene transfer by an adeno-associated virus (AAV) vector. *Brain Res* **713**: 99–107.
- Mandel, RJ, Rendahl, KG, Spratt, SK, Snyder, RO, Cohen, LK and Leff, SE (1998). Characterization of intrastriatal recombinant adeno-associated virus-mediated gene transfer of human tyrosine hydroxylase and human GTP-cyclohydrolase I in a rat model of Parkinson's disease. *J Neurosci* **18**: 4271–4284.
- During, MJ *et al.* (1998). *In vivo* expression of therapeutic human genes for dopamine production in the caudates of MPTP-treated monkeys using an AAV vector. *Gene Ther* **5**: 820–827.
- Skorupa, AF, Fisher, KJ, Wilson, JM, Parente, MK and Wolfe, JH (1999). Sustained production of beta-glucuronidase from localized sites after AAV vector gene transfer results in widespread distribution of enzyme and reversal of lysosomal storage lesions in a large volume of brain in mucopolysaccharidosis VII mice. *Exp Neurol* **160**: 17–27.
- Bosch, A, Perret, E, Desmaris, N and Heard, JM (2000). Long-term and significant correction of brain lesions in adult mucopolysaccharidosis type VII mice using recombinant AAV vectors. *Mol Ther* **1**: 63–70.
- Frisella, WA *et al.* (2001). Intracranial injection of recombinant adeno-associated virus improves cognitive function in a murine model of mucopolysaccharidosis type VII. *Mol Ther* **3**: 351–358.
- Passini, MA *et al.* (2005). AAV vector-mediated correction of brain pathology in a mouse model of Niemann-Pick A disease. *Mol Ther* **11**: 754–762.
- De, BP *et al.* (2006). High levels of persistent expression of alpha1-antitrypsin mediated by the nonhuman primate serotype rh.10 adeno-associated virus despite preexisting immunity to common human adeno-associated viruses. *Mol Ther* **13**: 67–76.
- Nguyen, JB, Sanchez-Pernaute, R, Cunningham, J and Bankiewicz, KS (2001). Convection-enhanced delivery of AAV-2 combined with heparin increases TK gene transfer in the rat brain. *Neuroreport* **12**: 1961–1964.
- Mastakov, MY, Baer, K, Symes, CW, Leichtlein, CB, Kotin, RM and During, MJ (2002). Immunological aspects of recombinant adeno-associated virus delivery to the mammalian brain. *J Virol* **76**: 8446–8454.
- Fu, H *et al.* (2003). Self-complementary adeno-associated virus serotype 2 vector: global distribution and broad dispersion of AAV-mediated transgene expression in mouse brain. *Mol Ther* **8**: 911–917.
- Cressant, A *et al.* (2004). Improved behavior and neuropathology in the mouse model of Sanfilippo type IIIB disease after adeno-associated virus-mediated gene transfer in the striatum. *J Neurosci* **24**: 10229–10239.
- Desmaris, N, Verot, L, Puech, JP, Caillaud, C, Vanier, MT and Heard, JM (2004). Prevention of neuropathology in the mouse model of Hurler syndrome. *Ann Neurol* **56**: 68–76.
- Lin, D *et al.* (2005). AAV2/5 vector expressing galactocerebrosidase ameliorates CNS disease in the murine model of globoid-cell leukodystrophy more efficiently than AAV2. *Mol Ther* **12**: 422–430.
- Broekman, ML, Comer, LA, Hyman, BT and Sena-Estevés, M (2006). Adeno-associated virus vectors serotyped with AAV8 capsid are more efficient than AAV-1 or -2 serotypes for widespread gene delivery to the neonatal mouse brain. *Neuroscience* **138**: 501–510.
- Klein, RL, Dayton, RD, Leidenheimer, NJ, Jansen, K, Golde, TE and Zweig, RM (2006). Efficient neuronal gene transfer with AAV8 leads to neurotoxic levels of Tau or green fluorescent proteins. *Mol Ther* **13**: 517–527.
- Cearley, CN and Wolfe, JH (2006). Transduction characteristics of adeno-associated virus vectors expressing cap serotypes 7, 8, 9, and Rh10 in the mouse brain. *Mol Ther* **13**: 528–537.
- Kaspar, BK, Erickson, D, Schaffer, D, Hinh, L, Gage, FH and Peterson, DA (2002). Targeted retrograde gene delivery for neuronal protection. *Mol Ther* **5**: 50–56.
- Passini, MA, Lee, EB, Heuer, GG and Wolfe, JH (2002). Distribution of a lysosomal enzyme in the adult brain by axonal transport and by cells of the rostral migratory stream. *J Neurosci* **22**: 6437–6446.
- Hackett, NR *et al.* (2005). Safety of direct administration of AAV2(CU)hCLN2, a candidate treatment for the central nervous system manifestations of late infantile neuronal ceroid lipofuscinosis, to the brain of rats and nonhuman primates. *Hum Gene Ther* **16**: 1484–1503.
- Halbert, CL *et al.* (2006). Prevalence of neutralizing antibodies against adeno-associated virus (AAV) types 2, 5, and 6 in cystic fibrosis and normal populations: implications for gene therapy using AAV vectors. *Hum Gene Ther* **17**: 440–447.
- Manno, CS *et al.* (2006). Successful transduction of liver in hemophilia by AAV-Factor IX and limitations imposed by the host immune response. *Nat Med* **12**: 342–347.
- Sleat, DE *et al.* (2004). A mouse model of classical late-infantile neuronal ceroid lipofuscinosis based on targeted disruption of the CLN2 gene results in a loss of tripeptidyl-peptidase I activity and progressive neurodegeneration. *J Neurosci* **24**: 9117–9126.
- Griffey, M *et al.* (2004). Adeno-associated virus 2-mediated gene therapy decreases autofluorescent storage material and increases brain mass in a murine model of infantile neuronal ceroid lipofuscinosis. *Neurobiol Dis* **16**: 360–369.
- Griffey, MA *et al.* (2006). CNS-directed AAV2-mediated gene therapy ameliorates functional deficits in a murine model of infantile neuronal ceroid lipofuscinosis. *Mol Ther* **13**: 538–547.
- Daly, TM, Vogler, C, Levy, B, Haskins, ME and Sands, MS (1999). Neonatal gene transfer leads to widespread correction of pathology in a murine model of lysosomal storage disease. *Proc Natl Acad Sci USA* **96**: 2296–2300.
- Butman, BT *et al.* (2006). Comprehensive characterization of the 293-ORF6 cell line. *Dev Biol Basel* **123**: 225–233.

36. De, B *et al.* (2004). Intrapleural administration of a serotype 5 adeno-associated virus coding for alpha1-antitrypsin mediates persistent, high lung and serum levels of alpha1-antitrypsin. *Mol Ther* **10**: 1003-1010.
37. Gao, GP, Alvira, MR, Wang, L, Calcedo, R, Johnston, J and Wilson, JM (2002). Novel adeno-associated viruses from rhesus monkeys as vectors for human gene therapy. *Proc Natl Acad Sci USA* **99**: 11854-11859.
38. Lin, L and Lobel, P (2001). Production and characterization of recombinant human CLN2 protein for enzyme-replacement therapy in late infantile neuronal ceroid lipofuscinosis. *Biochem J* **357**: 49-55.
39. Peterson, DA, Dickinson-Anson, HA, Leppert, JT, Lee, KF and Gage, FH (1999). Central neuronal loss and behavioral impairment in mice lacking neurotrophin receptor p75. *J Comp Neurol* **404**: 1-20.
40. Kida, E, Golabek, AA, Walus, M, Wujek, P, Kaczmarek, W and Wisniewski, KE (2001). Distribution of tripeptidyl peptidase I in human tissues under normal and pathological conditions. *J Neuropathol Exp Neurol* **60**: 280-292.
41. Hackett, NR *et al.* (2000). Use of quantitative TaqMan real-time PCR to track the time-dependent distribution of gene transfer vectors *in vivo*. *Mol Ther* **2**: 649-656.